The checkerboard update Glauber model, cellular automata and Ising models

1990 J. Phys. A: Math. Gen. 23 4165

(http://iopscience.iop.org/0305-4470/23/18/021)

J. Phys. A: Math. Gen. 23 (1990) 4165-4181. Printed in the UK

The checkerboard update Glauber model, cellular automata and Ising models

H Fried†

Department of Physics FM-15, University of Washington, Seattle WA 98195, USA

Received 2 May 1990

Abstract. The checkerboard update Glauber model for the one-dimensional Ising model is mapped onto a cellular automata model. This cellular automata model is found to be a special case of the well known (two-state) triangular cellular automata model. We show, therefore, that there exists a subspace of the full parameter space of the triangular cellular automata that obeys detailed balance. Using this result we show that there are no phase transitions within the interior of the cubical parameter space of the triangular cellular automata model. We identify a new line of critical points for the triangular cellular automata. This critical line is associated with the zero-temperature critical line of the one-dimensional Ising antiferromagnetic in an external field. The critical properties of the checkerboard Glauber model are studied and are found to be identical to those of the single-spin update model. In addition, the correlations in the checkerboard Glauber model are found to exhibit a null-cone structure, similar to that found in relativity theory. This null-cone, which originates in the constraints imposed by the checkerboard update procedure, is found to be a general property of the triangular cellular automata model.

1. Introduction

The present work is devoted to the study of the one-dimensional checkerboard update Glauber model and its relationship to particular one-dimensional cellular automata and two-dimensional Ising models. The one-dimensional Glauber model [1] can be used to model the kinetic properties of the one-dimensional q-state Potts models. The static (i.e. equilibrium) properties of these latter models are known exactly [2]. The present discussion focuses on the $q = 2$ ferromagnetic and antiferromagnetic nearest-neighbour Potts model (i.e. the Ising model) in an external field; the results, however, are easily generalized to the q-state Potts models [3]. Our results are obtained by first mapping the checkerboard update Glauber model onto a one-dimensional two-state cellular automata [4]. We then make use of the well known relationship [5, 6, 7] between one-dimensional cellular automata and two-dimensional Ising models to show that the parameter space of the checkerboard update Glauber model is equivalent to a subspace of the cellular automata model studied previously by Domany and Kinzel [5] and Choi and Huberman [3]. We shall call this model the triangular cellular automata. In particular these results allow a more complete understanding of the cubical parameter space of this cellular automata model. As is well known, Domany [8], using a special case of the mapping to be considered here, has been able to show

† Present address: Institut fur Physik, Johannes-Gutenberg Universitat and The Max Planck Institut fur Polymerforschung, D-6500 Mainz, Federal Republic of Germany.

0305-4470/90/184165+17$03.50

that the checkerboard update Glauber model in zero field is equivalent to the anisotropic triangular Ising model at its disorder point [9]. Exact results are known for the correlations functions of this triangular Ising model [9], which we employ to study the spacetime correlations in both the checkerboard Glauber model and triangular cellular automata.

Our results have the following consequences: we obtain exact information concerning the dynamic critical properties of the one-dimensional checkerboard update Glauber model. The checkerboard update procedure is important as it is used in vectorized Monte Carlo algorithms [10]. We show explicitly that the parameter space of the triangular cellular automata model contains a subspace which possesses the property of detailed balance [11]. This is especially interesting because using either the master-equation [3] or Ising model [5] formulation, one cannot determine whether a given cellular automata model obeys this important property. In addition, within these formulations, if the model does obey detailed balance, the time-slice Hamiltonian that would determine the temporal development of the system is completely unknown. For our special case we show that this time-slice Hamiltonian is the one-dimensional Ising Hamiltonian. Furthermore as the checkerboard Glauber model is shown to be equivalent to the triangular cellular automata, we identify a new line of critical points for the latter model. This critical line is associated with the zero-temperature critical line of the one-dimensional Ising antiferromagnet in an external field. Finally we can work backwards from the static properties of the one-dimensional Ising model (which are trivially known) and gain new information concerning the properties of the associated triangular cellular automata and two-dimensional Ising models.

The organization of this paper is as follows. In section 2 we define the checkerboard update Glauber model. In section 3 we map this model onto a two-dimensional triangular Ising model and show the equivalence between the checkerboard Glauber model and the triangular cellular automata. In section 4 we discuss the phase diagram of the Glauber model in the context of the larger parameter space of the two-state triangular cellular automata. In section 5 we discuss the correlation functions and critical properties.

2. The checkerboard update Glauber model

The checkerboard update Glauber model is defined as follows: consider a two-dimensional square spacetime lattice (figure 1(*a*)) in which on each site of the lattice sites an Ising spin $s(n, t) = \pm 1$. The time slices of the system consist of one-dimensional chains of spins which we label,

$$S(t) = (s(1, t), s(2, t), \ldots, s(N, t)). \tag{1}$$

The time-slice Hamiltonian is that of the one-dimensional nearest-neighbour Ising model in an external field,

$$-\beta H = J \sum_n s(n, t)s(n+1, t) + H \sum_n s(n, t). \tag{2}$$

The coupling J may be either ferromagnetic ($J > 0$) or antiferromagnetic ($J < 0$). To determine the temporal development of the system we employ a discrete-time master equation [11, 12],

$$P(S|t+1) = \sum_{\{S'\}} T_t(S|S')P(S'|t) \tag{3}$$

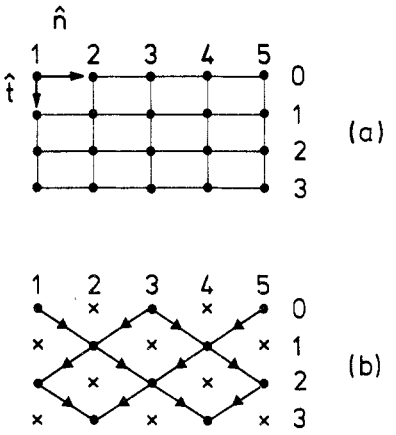

Figure 1. (*a*) The square spacetime lattice. ***n*** and ***t*** are unit vectors directed along the space and time directions respectively. In (*b*) the arrows along the diagonal lines indicate that the state of the pair of spins labelled by points are involved in the update of the spin labelled by a cross.

where $P(S|t)$ is the probability that at time t the system is in the microscopic state $S = S(t)$. $T_t(S|S')$ is the transfer matrix that determines the transition rates between the various microscopic states. We also impose the normalization conditions $\Sigma_s P(S|t) = 1$ and $\Sigma_s T(S|S') = 1$; the latter condition ensures conservation of probability. Using a checkerboard update procedure [12] (figure 1(*b*)) we may factorize the transfer matrix into local transfer matrices as

$$t_t(S|S') = \Pi'_n t(s(n-1), s(n), s(n+1)|s'(n)) \tag{4}$$

where the prime indicates that if t = even (odd) then the product is taken for n = even (odd). To make this a Glauber model we choose the local transfer matrices to have the form

$$t(s_1, s, s_2|-s) = \tfrac{1}{2}(1 - s\gamma_0) \qquad s_1 + s_2 = 0 \tag{5a}$$

$$t(s_1, s, s_2|-s) = \tfrac{1}{2}(1 - s\gamma_2) \qquad s_1 + s_2 = 2 \tag{5b}$$

$$t(s_1, s, s_2|-s) = \tfrac{1}{2}(1 + s\gamma_{-2}) \qquad s_1 + s_2 = -2 \tag{5c}$$

where $\gamma_0 = \tanh(H)$, $\gamma_2 = \tanh(2J + H)$ and $\gamma_{-2} = \tanh(2J - H)$. We furthermore impose the normalization condition,

$$t(s_1, s, s_2|s) = 1 - t(s_1, s, s_2|-s). \tag{6}$$

This choice for the local transfer matrix is equivalent to that employed (with $H = 0$) in the single-spin update model [1]. In addition we are ensured that our transfer matrix (4) generates a time development that obeys detailed balance because this property implicit in the local transfer matrix [1] is not altered by the checkerboard update procedure.

3. Mapping onto a triangular Ising model

Equations (2)-(5) constitute the definition of a one-dimensional two-state cellular automata model (i.e. both the microscopic system states and the spacetime are discrete).

In general such a model maps onto an anisotropic Ising model defined on a *square lattice* [5]. As Domany has shown [8], however, the checkerboard Glauber model defined above actually maps to an Ising model on a *triangular lattice.* It should be noted here that in Glauber's notation [1] (and with $H=0$) we have chosen the $\alpha=\frac{1}{2}$ and $\delta=0$ form for the local transfer matrices. Other choices [13, 14] for α and δ can be made. These more general local transfer matrices, however, can be shown to map onto a square-lattice Ising model. For purposes of simplicity and to make contact with previous work we will limit our discussion to the form chosen in [5].

We first rewrite the local transfer matrix in the form

$$t(s_1, s, s_2|s') = e^{H(s_1, s, s_2|s')}. \tag{7}$$

The Hamiltonian $H(s_1, s, s_2|s')$ is an Ising Hamiltonian defined on the plaquette shown in figure 2(a). Using the symmetry

$$t(s_1, s, s_2|s') = t(s_2, s, s_1|s') \tag{8}$$

which follows from the form of the spin coupling in the underlying one-dimensional Ising Hamiltonian, we find the most general plaquette Hamiltonian to be

$$\begin{aligned} H(s_1, s, s_2|s') &= N_0 + B_1(s_1+s_2) + Bs + B's' + K_1 s(s_1+s_2) + K_2 s_1 s_2 + K_3 s'(s_1+s_2) \\ &\quad + K_4 ss' + L_1 ss_1 s_2 + L_2 s' s_1 s_2 + L_3 ss'(s_1+s_2) + M_1 ss' s_1 s_2. \end{aligned} \tag{9}$$

In figure 2(b) some of these interactions are explicitly shown. Using (5) and (6) we find, after some lengthy algebra, that $B = K_1 = K_4 = L_1 = L_3 = M_1 = 0$. Therefore we are left with a Hamiltonian of the form

$$H(s_1, s, s_2|s') = N_0 + B_1(s_1+s_2) + B's' + K_2 s_1 s_2 + K_3 s'(s_1+s_2) + L_2 s' s_1 s_2. \tag{10}$$

If we define

$$p_0 = \tfrac{1}{2}(1-\gamma_{-2}) \tag{11a}$$

$$p_1 = \tfrac{1}{2}(1+\gamma_0) \tag{11b}$$

$$p_2 = \tfrac{1}{2}(1+\gamma_2) \tag{11c}$$

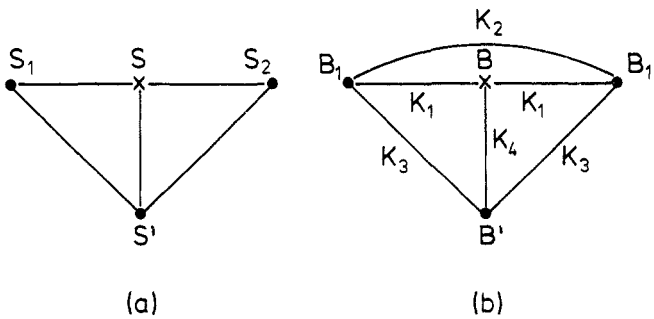

Figure 2. (a) The plaquette of spins involved in the definition of the local transfer matrix. The spin state s at time t is updated to the spins state s' at time $t+1$. (b) Some of the spin couplings involved in the definitions of (7) and (9).

we find that

$$e^{8B_1} = \frac{p_2(1-p_2)}{p_0(1-p_0)} \tag{12a}$$

$$e^{8B'} = \frac{p_0 p_1^2 p_2}{(1-p_0)(1-p_1)^2(1-p_2)} \tag{12b}$$

$$e^{8K_2} = \frac{p_0(1-p_0)p_2(1-p_2)}{p_1^2(1-p_1)^2} \tag{12c}$$

$$e^{8K_3} = \frac{p_2(1-p_0)}{p_0(1-p_2)} \tag{12d}$$

$$e^{8L_2} = \frac{p_0(1-p_1)^2 p_2}{p_1^2(1-p_0)(1-p_2)} \tag{12e}$$

$$e^{8N_0} = p_0(1-p_0)p_1^2(1-p_1)^2 p_2(1-p_2). \tag{12f}$$

Equations (10) and (12) are exactly those found by Domany and Kinzel [5] in the study of the triangular cellular automata model. The important result to note is that $H(s_1, s, s_2|s') = H(s_1, s_2|s')$; all dependence on s has dropped out. This would not have been the case if we had chosen $\alpha \neq \frac{1}{2}$ or $\delta \neq 0$. Therefore the plaquete Hamiltonian couples the spins located on the vertices of the down triangle (see figure 3(a)). The total transition probability defined by

$$\begin{aligned} P(S|T) &= \sum_{\{s(n,t)\}} T_{T-1}(S|S_{T-1}) T_{T-2}(S_{T-1}|S_{T-2}) \ldots T_1(S_1|S') P(S'|0) \\ &= \sum_{\{s(n,t)\}} e^{H[(s(n,t))]} P(S'|0) \end{aligned} \tag{13}$$

therefore corresponds to the partition function for the two-dimensional triangular Ising model with the Hamiltonian (see figure 3(b)),

$$\begin{aligned} H(\{s(n,t)\}) = B \sum_r s(r) + K_2 \sum_{\langle r,r' \rangle}^{(H)} s(r)s(r') \\ + K_3 \sum_{\langle r,r' \rangle}^{(D)} s(r)s(r') + L_2 \sum_{\langle r,r',r'' \rangle}^{(\triangle)} s(r)s(r')s(r''). \end{aligned} \tag{14}$$

Note that we have dropped the constant term and $B = B' + 2B_1$. The symbols (H), (D) and ($\triangle$) respectively represent sums restricted to the horizontal, diagonal and down

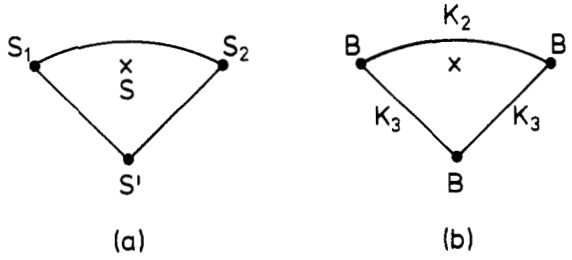

Figure 3. (a) The spins connected by lines are those that remain in the definition of the local transfer matrix when the constraints in (5) and (6) are applied. (b) The associated ising interactions that remain non-zero (the three spin interaction L_2 is not shown).

pointing triangles of the triangular lattice. The coordinate labels $r = (n, t)$ are now the coordinate labels restricted to those sites corresponding to the triangular sub-lattice of the full square spacetime lattice.

To define the cellular automata associated with the checkerboard Glauber model we employ the definitions in (5) and (11) to write:

$$t(-1, -1|1) = p_0 \tag{15a}$$

$$t(1, -1|1) = t(-1, 1|1) = p_1 \tag{15b}$$

$$t(1, 1|1) = p_2. \tag{15c}$$

We have dropped explicit reference to the spin s and so have written the local transfer matrix as $t(s_1, s_2|s')$. For arbitrary values of $0 \leqslant p_0, p_1, p_2 \leqslant 1$, these transition probabilities define the well known (two-state) triangular cellular automata. We, however, consider only a subspace of this parameter space because the probabilities p_0, p_1, p_2 are not independent, our model having only the two free parameters J and H. It should be noted here that (2) is the most general one-dimensional Ising Hamiltonian which maps onto a triangular Ising model. For example, with the inclusion of second-neighbour interactions our Glauber model would not map onto a two-dimensional triangular Ising model and so would not be contained in the cellular automata model defined by (15). By implication the triangular cellular automata model will not have a well-defined time-slice Hamiltonian outside the parameter range of the Glauber model. Therefore we claim to have found the only subspace of the triangular cellular automata model that obeys detailed balance.

In the sections which follow we will discuss the phase diagram and correlation functions of the checkerboard Glauber model. We will also discuss in detail, its relationship to the triangular cellular automata model and the associated two-dimensional triangular Ising model.

4. Phase diagram of the triangular cellular automata

As we have previously shown, the checkerboard Glauber model, when formulated as a cellular automata, corresponds to a subspace of the (p_0, p_1, p_2) parameter space of the triangular cellular automata. This larger parameter space forms a cube defined by, $0 \leqslant p_0, p_1, p_2 \leqslant 1$ (see figure 4). To study the symmetries of this model we redefine the origin of coordinates as the centre of this cube. Hence,

$$t(-1, -1|1) = p_0 = \tfrac{1}{2} + \varepsilon_0 \tag{16a}$$

$$t(1, -1|1) = t(-1, 1|1) = p_1 = \tfrac{1}{2} + \varepsilon_1 \tag{16b}$$

$$t(1, 1|1) = p_2 = \tfrac{1}{2} + \varepsilon_2. \tag{16c}$$

Under a spin-flip transformation, which relabels the spin states yet leaves the properties of the model unchanged, we have

$$t(1, 1|-1) = 1 - p_2 = \tfrac{1}{2} - \varepsilon_2 \tag{17a}$$

$$t(1, -1|1) = t(-1, 1|1) = 1 - p_1 = \tfrac{1}{2} - \varepsilon_1 \tag{17b}$$

$$t(1, 1|1) = 1 - p_0 = \tfrac{1}{2} - \varepsilon_0. \tag{17c}$$

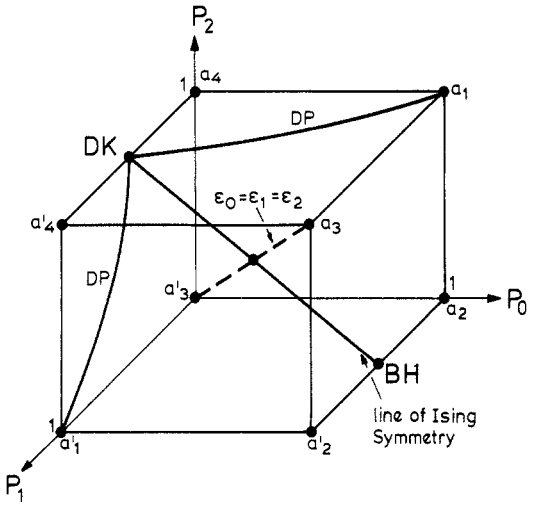

Figure 4. The cubical parameter space of the triangular cellular automata. The vertices a_i map into a_i' under the spin-inversion transformation.

Therefore under this transformation,

$$(\varepsilon_0, \varepsilon_1, \varepsilon_2) \rightarrow (-\varepsilon_2, -\varepsilon_1, -\varepsilon_0). \tag{18}$$

The subspace invariant under this transformation (i.e. the subspace with Ising symmetry) defines the line $\varepsilon_1 = 0$, $\varepsilon_0 = -\varepsilon_2$ (or $p_1 = \frac{1}{2}$, $p_0 = 1 - p_2$). We shall see that this line corresponds to the zero-field Glauber model. Equation (18) shows that it is sufficient to consider the properties of only half of the cubical parameter space. In figure 4 the cubical parameter space and the mappings of the vertices are shown. The line of Ising symmetry which connects the points labeled DK (Domany-Kinzel) and BH (Blöte-Hilhorst) is also shown. The lines located on the $(p_0 = 0, p_1, p_2)$ and $(p_0, p_1, p_2 = 1)$ faces denote the phase boundaries for the generalized directed percolation models which have been studied in detail by Domany and Kinzel [5] and Kinzel [12]. The structure of the upper face follows from the symmetry under the transformation defined in (18). For the remainder of this section our aim is to discuss how the checkerboard Glauber model fits into this parameter space. We also use the known properties of the equilibrium state of the Glauber model (i.e. the equilibrium state of the one-dimensional Ising model) to infer additional properties of the triangular cellular automata.

First consider the Glauber model in zero-field (i.e. $H = 0$). Using (11) we find that $p_0 = 1 - p_2$ and $p_1 = \frac{1}{2}$; this, therefore, corresponds to the line of Ising symmetry. Using (12) we find that $B = L_2 = 0$ and $K_3 = J$, $K_2 = -\frac{1}{2}\ln[\cosh(2J)]]$. The latter two equations lead to the result found first by Domany [8]:

$$e^{-2K_2} = \cosh(2K_3). \tag{19}$$

This equation identifies the line of Ising symmetry as that of the disorder point of the nearest-neighbour anisotropic triangular Ising model [8]. Therefore, by implication, the zero-field checkerboard model is also equivalent to the disorder point of this triangular Ising model. In the context of the cellular automata models, this was first noted by Domany and Kinzel [5]. It should be noted, however, that the connection between the checkerboard Glauber model and the triangular cellular automata model

was not made in this latter work. A similar result was found by Peschel and Emergy [15] in the context of the single-spin update Glauber model.

To study the case $H \neq 0$ of the checkerboard update Glauber model we write,

$$2\varepsilon_0 = \tanh(H - 2J) \tag{20a}$$

$$2\varepsilon_1 = \tanh(H) \tag{20b}$$

$$2\varepsilon_2 = \tanh(H + 2J). \tag{20c}$$

With $J = 0$ and H arbitrary (which corresponds to the one-dimensional Ising model at $T = \infty$) we find the associated line $\varepsilon_0 = \varepsilon_1 = \varepsilon_2$. The equilibrium phase diagram of the one-dimensional Ising model is shown in figure 5. In this figure we also show those points on the phase diagram which correspond to particular vertices of the cubical parameter space (see also figure 4). At $J = \infty$ and $H = 0$ there is a ferromagnetic transition, whereas for $J = -\infty$ the entire $(-\infty, H)$ line is critical because the external field is irrelevant (in the renormalization group sense) for the Ising antiferromagnet. It follows that under the mapping defined in (20) we should expect to find a critical point located at $(\varepsilon_0 = -\frac{1}{2},\ \varepsilon_1 = 0,\ \varepsilon_2 = \frac{1}{2})$ associated with the zero-temperature ferromagnetic transition. This transition has been previously studied by Domany and Kinzel [5] in the context of the generalized directed percolation models. They consider the triangular cellular automata model along the line $-\frac{1}{2} \leqslant \varepsilon_1 \leqslant \frac{1}{2}$ and $-\varepsilon_0 = \varepsilon_2 = \frac{1}{2}$. This corresponds to the zero-temperature one-dimensional Ising ferromagnetic as a function of the external field (i.e. $J = -\infty$, $-\infty \leqslant H \leqslant \infty$). The critical point corresponds to $H = 0$. We also expect to find a line of critical points located at $-\frac{1}{2} \leqslant \varepsilon_1 \leqslant \frac{1}{2}$ and $\varepsilon_0 = -\varepsilon_2 = \frac{1}{2}$ associated with the zero-temperature antiferromagnetic transition. This critical line is a new feature to be found in the triangular cellular automata model. The parameter range over which the full Glauber model is defined is shown in cross section in figure 6.

Let us now turn to a more detailed examination of the critical points. As discussed by Domany and Kinzel [5] the ferromagnetic critical point can be interpreted as a model of vicious random walkers. At this critical point the local transfer matrix is characterized by $p_0 = 0$ and $p_2 = 1$. Therefore (-1)-domains ((1)-domains) transform in one time step into (-1)-domains ((1)-domains). At $p_1 = \frac{1}{2}$ the domain walls between

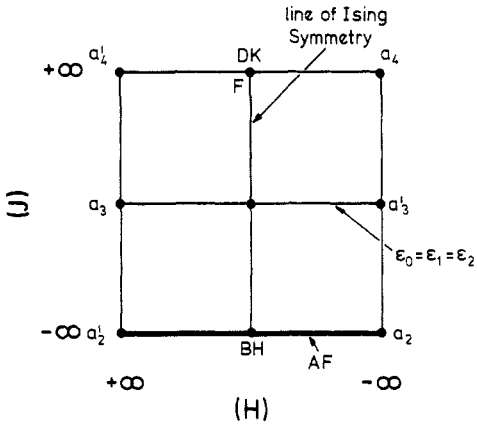

Figure 5. The phase diagram of the one-dimensional Ising model. The line labelled AF is the antiferromagnetic critical line. Also shown are those points labelled a_i that correspond to the vertices of the cubical parameter space.

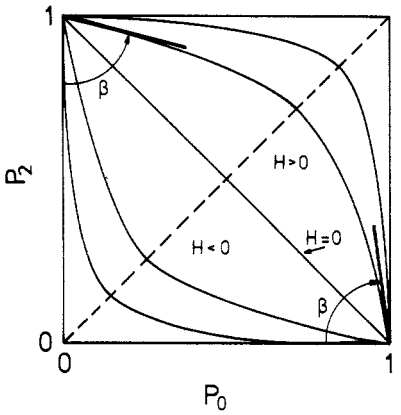

Figure 6. The projection of the subspace of the Glauber model onto the (p_0, p_2) plane. The line $H = 0$ corresponds to the line of Ising symmetry ($p = \frac{1}{2}$). The angle β is defined by the relationship $\tan \beta = e^{4H}$.

these domains can move to the right or left with equal probability ($=\frac{1}{2}$). Therefore these domain walls execute a random walk. When two domain walls meet they anihilate one another (see figure 7), and so these are vicious random walkers.

We can interpret the antiferromagnetic critical line in a similar manner. Along the this line $p_0 = 1$ and $p_2 = 0$ and so (-1)-domains ((1)-domains) transform in one time step into (1)-domains ((−1)-domains). Along the critical line p_1 varies within the range, $0 \leqslant p_1 \leqslant 1$, and so the domain walls hop to the left or right with a rate determined by the specific value of p_1. The situation is complicated in that the (-1)-domains and (1)-domains interchange after each time step. To see the character of the domain wall excitations we must consider a two-step transformation (see figure 8). Consider a single domain wall with a (1)-domain to the left and a (-1)-domain to the right. This domain wall hops one step to the left (figure 8(a)) with a probability $p_1(1-p_1)$ if a $(+,-) \rightarrow +$ transformation is followed by a $(-,+) \rightarrow -$ transformation. If these transformations are done in reverse order it hops one step to the right (figure 8(b)) with a probability $(1-p_1)p_1$. The domain wall remains stationary (figure 8(c) and (d)) if either of the transformation sequences $(+,-) \rightarrow +$ and $(-,+) \rightarrow +$ or $(+,-) \rightarrow -$ and $(-,+) \rightarrow -$ occur. The total probability for the domain wall to remain stationary is $p_1^2 + (1-p_1)^2$.

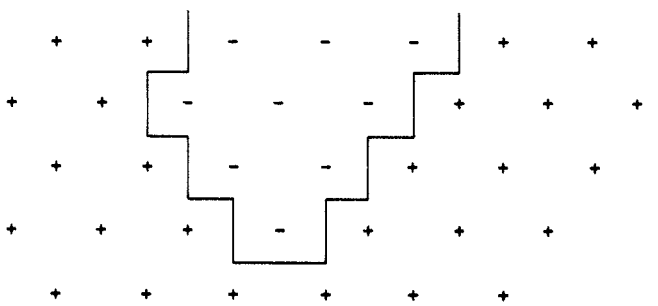

Figure 7. An example of two viscious randomly-walking domain walls at the ferromagnetic critical point.

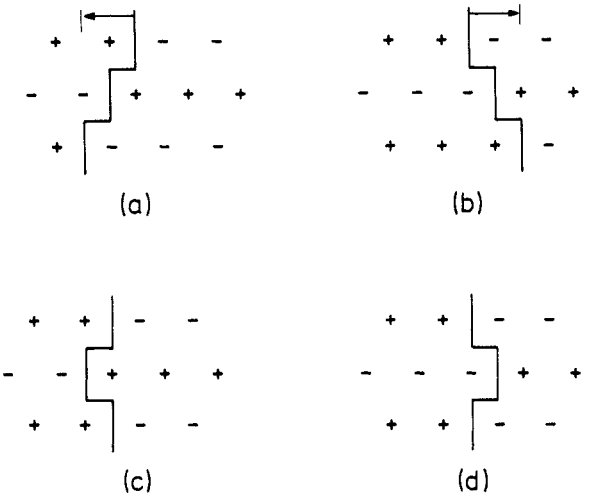

Figure 8. The two-step transformation at the antiferromagnetic critical point. (*a*) and (*b*) have probabilities $p_1(1-p_1)$, (*c*) p_1^2 and (*d*) $(1-p_1)^2$.

The picture is similar if the (± 1)-domains are initially reversed; here, however, the order in which the transformations occur must also be reversed. As the two-step domain wall hopping probabilities for this model are symmetric with respect to left and right hopping, we therefore have a (vicious) random walk model for the entire critical line. The property that distinguishes the points along this line is the self-diffusion coefficient D of the walkers, where,

$$D = 2[p_1(1-p_1)]^{1/2}. \tag{21}$$

Because this coefficient is non-universal we do not expect that it will affect the critical properties along this line (i.e. the p_1-direction is irrelevant).

It is interesting to note that at the point $\varepsilon_0 = \frac{1}{2}$, $\varepsilon_1 = 0$ and $\varepsilon_2 = -\frac{1}{2}$ the couplings for the associated two-dimensional triangular Ising model take the form $B = L_2 = 0$ and $K_2 - K_3 = \frac{1}{2}\ln\frac{1}{2} = \Delta_c$. This value of Δ_c corresponds precisely to the transition point in the roughening model studied by Blöte and Hilhorst [16]. For this reason we have labelled this point the BH point. They, however, chose a different cut through the parameter space in which $K_2, K_3 \to -\infty$ and Δ was allowed to vary.

We have shown that the phase diagram of the one-dimensional Ising model is embedded within the cubical parameter space of the triangular cellular automata. Therefore the existence of critical points in the one-dimensional Ising model implies that associated critical points are present in the triangular cellular automata. In addition we note that all of the critical points so far (including the generalized directed percolation transitions) are confined to the faces (and edges and vertices) of the cube.

We claim that there are no phase transitions (i.e. critical points) in the interior of the cube. Let us first restrict attention to the $p_1 = \frac{1}{2}$ plane of the cubical parameter space (see figure 6). Within this plane the line $p_0 = 1 - p_2$, corresponds to the zero-field Glauber model. The endpoints of this line correspond to the zero-field critical points of the one-dimensional Ising model. The line $p_0 = p_2$ divides the plane into a 'ferromagnetic' region where $p_0 < p_2$ and an 'antiferromagnetic' region where $p_0 > p_2$. As p_1 $(=\frac{1}{2})$ is constant throughout the entire plane we know that the domain wall excitations have

the same character for each point in the plane. Because the endpoints of the Glauber line are random walk points, the structure here is like that of the uniaxially incommensurate (striped) critical phase of the Pokrovsky-Talpov model [17]. Moving away from these points along the Glauber line we know from the exact solution of the one-dimensional Ising model that there is a finite correlation length. The system therefore is no longer critical. The general form of the excitations introduced in moving away from the critical points is shown in figure 9. These are dislocations similar to those responsible for producing the disordered fluid in the models of commensurate-incommensurate phase transitions [18]. The feature which distinguishes the Glauber line from the remainder of the plane is that there exists an explicit relationship between the core energy of the dislocations and the values of the Ising couplings H and J. If we move off the Glauber line while remaining in the plane, we retain the dislocation excitations; we merely lose the dependence of the core energy on the couplings J and H. Because the precise value of the core energy is irrelevant, the entire ($p_1 = \frac{1}{2}$) plane (away from the edges) is also non-critical. The argument for arbitrary p_1 and $p_2 < p_1$ (i.e. in the antiferromagnetic region) is exactly the same, as the antiferromagnetic critical line is also a random walk point.

The argument for the ferromagnetic region with $p_1 \neq \frac{1}{2}$ is similar to the one presented above. We know that at the endpoint of the Glauber line the correlation length is finite (i.e. this corresponds to $J = \infty$, $H \neq 0$). As we move away from this point along the Glauber line we introduce dislocations similar to those of the two-dimensional Ising ferromagnet in an external field. However, because these domain walls are not random walkers (i.e. $p_1 \neq \frac{1}{2}$), these dislocations have no effect on the critical properties of the model. If we move off the Glauber line we merely change the core energy of these dislocations. Therefore we have shown that throughout the interior of the cube the model is non-critical, and hence there are no phase transitions within this region.

We now turn to a discussion of the faces of the cube. The face ($p_0 = 0, p_1, p_2$) (and by symmetry ($p_0, p_1, p_2 = 1$)) has been studied by Domany and Kinzel [5] and is well understood. There are no phase transitions away from the antiferromagnetic critical line on the face ($p_0 = 1, p_1, p_2$) (and by symmetry ($p_0, p_1, p_2 = 0$)). This is so because the excitations introduced in moving away from the critical line on this face are the same dislocations as introduced upon moving to the interior of the cube. A difficulty

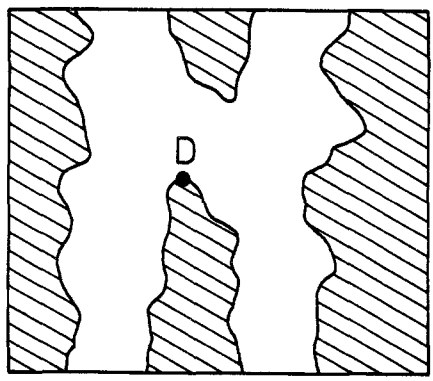

Figure 9. The general form of the dislocation excitations (originating at the spacetime point labelled D) for the randomly walking domain walls. The shaded and unshaded regions denote the two distinct types of domains.

occurs, however, as to the status of the point ($p_0 = 1, p_1 = 0, p_2 = 1$) (and by symmetry ($p_0 = 0, p_1 = 1, p_2 = 0$)) which corresponds, in Wolfram's notation [4], to the 165 deterministic cellular automata. It should be noted that Domany and Kinzel [5] are also uncertain of the properties of this point. Finally, for the face ($p_0, p_1 = 1, p_2$) (and by symmetry ($p_0, p_1 = 0, p_2$)) we have only a few remarks. We know that along the lines ($p_0 = 0, p_1 = 1, p_2$) (from Domany and Kinzel) and ($p_0, p_1 = 1, p_2 = 1$) and ($p_0 = 1, p_1 = 1, p_2$) (both from the Glauber model) there are no phase transitions. However, there are open questions along the line ($p_0, p_1 = 1, p_2 = 0$) and on the interior of the face. It is doubtful, however, that any further transitions will be found.

In summary, the symmetries of the cubical parameter space of the triangular cellular automata model have been discussed. It has been shown how the checkerboard Glauber model maps into this parameter space and a new line of critical points have been identified. This critical line is associated with the zero-temperature antiferromagnetic critical line of the one-dimensional Ising model. Our knowledge of the exact solution of the one-dimensional Ising model has also been used to gain further information concerning the properties of the triangular cellular automata model within the interior and the faces of the cube. We turn now to a discussion of the correlation functions and critical properties of these models.

5. Correlation functions and critical properties

In discussing the correlation functions of the checkerboard update Glauber model we note that under the mappings in (10) and (15) the correlation functions will be identical to those of the associated two-dimensional Ising model and triangular cellular automata for the parameter ranges of interest. In particular as

$$K_2 - K_3 = \frac{1}{4} \ln \left| \frac{p_0(1-p_2)}{p_1(1-p_1)} \right| \tag{22}$$

is generally not equal to zero the associated two-dimensional Ising model is anisotropic. This implies that the correlation functions will have the form

$$\langle s(n, t) s(n', t') \rangle = f(r, \theta) \tag{23}$$

where $r = [(n-n')^2 + (t-t')^2]^{1/2}$ and $\theta = 0$ in the direction parallel to the time axis (see figure 10). Note that we have written the coordinates (n, t) relative to the underlying

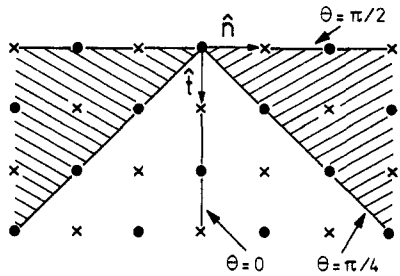

Figure 10. The null-cone $|\theta| = \pi/4$ for the checkerboard update models. $\theta = 0$ is directed along the time axis, $|\theta| = \varepsilon/2$ is directed along the space axis.

square spacetime lattice. When applied to the triangular Ising model we must impose the restriction n = even (odd) for t = even (odd).

As the Glauber model obeys detailed balance, we know that the *equilibrium* correlation function for $|\theta| = \pi/2$ (i.e. the correlation function within a time slice) is simply that of the equilibrium correlation function of the one-dimensional Ising model. Therefore we have

$$\langle s(n, t)s(n', t)\rangle = A\, \mathrm{e}^{-|n-n'|/\xi(|\theta|=\pi/2)} \tag{24}$$

where $A = 1$ for $J > 0$ and $A = (-1)^{|n-n'|}$ for $J < 0$. The explicit form of the perpendicular correlation length is the familiar result [2]

$$\xi^{-1}\left(|\theta| = \frac{\pi}{2}\right) = -\ln(|B|) \tag{25}$$

where

$$B = \frac{\mathrm{e}^{J}\cosh(H) - (\mathrm{e}^{-2J} + \mathrm{e}^{2J}\sinh^2(H))^{1/2}}{\mathrm{e}^{J}\cosh(H) + (\mathrm{e}^{-2J} + \mathrm{e}^{2J}\sinh^2(H))^{1/2}}. \tag{26}$$

For the special case $H = 0$ we find that $\xi^{-1}(|\theta| = \pi/2) = -\ln|\tanh(J)|$. As we have noted above, the line $H = 0$ (which is the line of Ising symmetry) is equivalent to the disorder line of the anisotropic (nearest-neighbour) triangular Ising model. The correlation functions of this model have been studied by Stephenson [9]. He found that along the $|\theta| = \pi/2$ direction $\xi^{-1} = -\ln|\tanh(K_2)|$. Using (19) this implies that

$$\tanh(K_2) = -\tanh^2(K_3) = -\tanh^2(J). \tag{27}$$

The last equality follows from the restriction to $H = 0$. Therefore $\xi^{-1} = -2\ln|\tanh(J)|$, which is equivalent to our result; the factor of two occurs in the latter case by the restriction to the sites of the triangular lattice. In addition to the $|\theta| = \pi/2$ direction, Stephenson also found an exact expression for the correlation function along the $|\theta| = \pi/4$ direction. Using our notation this result takes the form

$$\langle s(n, t)s(n + a, t + a)\rangle = \mathrm{e}^{-a/\xi} \tag{28}$$

where $\xi^{-1}(|\theta| = \pi/4) = -\ln|\tanh(J)|$ and a is an integer. Interestingly, the correlations are the same along the $|\theta| = \pi/2$ and $|\theta| = \pi/4$ directions. This result is to be expected as our checkerboard update procedure limits the temporal influence of one spin on another to exactly the line $|\theta| = \pi/4$. The line $|\theta| = \pi/4$, therefore, represents a 'null-cone' similar to that found in relativity theory [19]. We can now draw two conclusions. First the null-cone should be present for the entire parameter space of the triangular cellular automata as the checkerboard update scheme is used throughout. This result includes as special case the $H \neq 0$ Glauber model and the generalized directed percolation models. Second, the correlation length should obey

$$\xi(\theta) = \xi\left(\theta = \frac{\pi}{2}\right) \tag{29}$$

for all angles in the range $\pi/4 \leqslant |\theta| \leqslant \pi/2$. This latter result follows because these angles correspond to pairs of spins at a spacelike separation and so, by the above arguments, should not influence one another. Therefore, we have not only gained additional information concerning the correlations present in the Glauber model but

have extended this information to the entire parameter space of the triangular cellular automata. We should emphasize however that the explicit form of the null and spacelike correlation lengths is known only in the subspace of the Glauber model. For the remainder of the parameter space we have only the general result exhibited in (29).

We have not been able to find explicit expressions for the correlation functions along the directions $|\theta| < \pi/4$ (i.e. for spins at a time-like separation). In principle one can calculate these using the method of Pfaffians [9, 20], though the calculation is quite involved. We can, however, constrain the form of the correlation length $\xi(|\theta| < \pi/4)$ in the regions about the critical points. The argument goes as follows: we parametrize the path taken into the critical point (i.e. to any of the Ising critical points) by $\varepsilon = \varepsilon(p_0, p_1, p_2)$ where $\varepsilon = 0$ is the location of the critical point. We expect that for ε small the correlation length takes the scaling form

$$\xi\left(|\theta| \geqslant \frac{\pi}{4}\right) \approx \varepsilon^{-\nu} \tag{30}$$

and

$$\xi\left(|\theta| < \frac{\pi}{4}\right) \approx \varepsilon^{-\tau} \tag{31}$$

where $\nu = \nu(|\theta| = \pi/2)$ and $\tau = \tau(\theta = 0)$ are the correlation length exponents in the space and time directions respectively. That $\tau \neq \tau(\theta)$ follows from the fact that for $0 < |\theta| < \pi/4$ we expect the correlations to be a combination of the purely spatial correlations (controlled by ν) and the purely temporal correlations (controlled by τ). The θ dependence of $\xi(|\theta| < \pi/3)$, occurs only in a non-universal prefactor to the correlation length and so is irrelevant for ε small. We have made the implicit assumption (and one which we shall show to be correct) that

$$\tau \geqslant \nu \tag{32}$$

so that for small ε the divergence in the correlation length for $|\theta| < \pi/4$ is controlled by the exponent τ. If we can calculate τ, this constrains the form of the timelike correlations in the critical region. To calculate τ we will make use of the result from the dynamic scaling hypothesis [21]

$$\tau = z\nu \tag{33}$$

where z is the dynamic scaling exponent. We will now show that the exponents ν and z can be extracted from the results that have been presented above.

To extract the exponent ν we make use of the explicit form of the correlation length given in (26). Let us first study the ferromagnetic critical point located at $(p_0 = 0, p_1 = \frac{1}{2}, p_2 = 1)$. If we choose the path into this critical point parametrized by $\varepsilon = |p_1 - \frac{1}{2}|$ with $p_0 = 0$ and $p_2 = 1$ (which corresponds to $J = \infty$, $|H| \to 0$) we find that for small ε,

$$\xi\left(|\theta| \geqslant \frac{\pi}{4}\right) \approx \varepsilon^{-1} \tag{34}$$

and so along this direction $\nu = 1$. This result is in agreement with that found previously by Domany and Kinzel [5]. If we choose the path $p_1 = \frac{1}{2}$, $\varepsilon = p_0 = 1 - p_2$ (which corresponds to $H = 0$, $J \to \infty$) we find

$$\xi\left(|\theta| \geqslant \frac{\pi}{4}\right) \approx \varepsilon^{-1/2}. \tag{35}$$

and so along this direction $\nu = \frac{1}{2}$. We further argue that as the core energy of the dislocations is irrelevant (see section 4), *any* path chosen with $p_1 = \frac{1}{2}$ (i.e. $H = 0$) will yield the exponent $\nu = \frac{1}{2}$.

To study the antiferromagnetic critical line we choose the paths defined along the subspace of the Glauber model at fixed p_1 (i.e. fixed H). These paths meets the critical line at an angle β given by (see figure 6)

$$\tan(\beta) = e^{4H}. \tag{36}$$

A simple calculation shows that

$$\xi\left(|\theta| \geqslant \frac{\pi}{4}\right) \approx \varepsilon^{-1/2} \tag{37}$$

holds along the entire critical line, and so we find that $\nu = \frac{1}{2}$. As in the case of the ferromagnetic point we argue that because the core energy of the dislocations is irrelevant the correlation length exponent satisfies $\nu = \frac{1}{2}$ along *any* path (with $p_1 =$ constant) leading into the critical line (i.e. for arbitrary β). This latter result for the antiferromagnetic critical line (and the associated result for the ferromagnetic critical point) constrains the form of the spacelike correlations for the more general triangular cellular automata, (in addition for (29)), in the critical region. This gives additional information concerning the critical behaviour of the triangular cellular automata model. It should be noted here that (34), (35) and (37) hold also for the single-spin update Glauber model. This is so since both the checkerboard update and the single-spin update models share the same equilibrium structure in the space direction (i.e. they both obey detailed balance).

So far we have studied the static critical properties associated with the equilibrium solution for the time slices of the Glauber model (i.e. the equilibrium one-dimensional Ising model). In order to study the dynamic critical properties of this model (i.e. the dynamic exponent z) we must make specific the initial conditions that have been chosen. Generally one begins with an arbitrary initial condition (as in a Monte Carlo simulation) or a distribution of initial conditions $P(S|0)$ as in (13). In the discussion above involving the correlation functions, we have assumed that the system had already reached thermal equilibrium. This is equivalent to choosing as our initial condition the stationary Boltzman distribution for the one-dimensional Ising model. In our formulation this is equivalent to the free boundary conditions employed by Stephenson to study the associated two-dimensional Ising model. In contrast to this, our discussion in the previous section concerning the random walk properties of the critical points assumed implicitly that all initial conditions had equal weight. This accounts in the latter case for the presence of domain walls for $|J| = \infty$. With equilibrium boundary conditions these domain walls would be absent and the system would be completely ordered in either the ferromagnetic or antiferromagnetic ground state.

It is important to note that to study the critical point, the choice of 'equiprobable' initial conditions does not represent the equilibrium state. The random walkers that are present therefore represent the relaxational modes of the system. This is evident from the fact that the walkers are 'vicious'. It is, however, the properties of this relaxation that interest us; they characterize the *critical* relaxation of the model. To calculate the dynamic exponent z we make use of a variant of an argument first used by Cordery *et al* [13] for the single-spin update models. Consider a system whose spatial dimension has the linear size L. We begin with a random distribution of domain walls. Because these domain walls are vicious (i.e. they anihilate one another upon

meeting), the system will have achieved equilibrium in the time T that it takes one domain wall to walk across the spatial extent of the system. Because these walls are random walkers we have immediately that $L \approx T^{1/2}$ or

$$T \approx L^2. \tag{38}$$

This identifies the dynamic critical exponent as

$$z = 2 \tag{39}$$

a result in agreement with both the single-spin update model [13] and the results of Domany and Kinzel [5]. This result also justifies our assumption in (32). Using (33) and (39) we find

$$\tau = 2 \tag{40}$$

along the $J = \infty$, $|H| \to 0$ path to the ferromagnetic critical point, and

$$\tau = 1 \tag{41}$$

along the remainder of the paths considered for the ferromagnetic and antiferromagnetic critical points.

In summary we have shown that the critical properties of the checkerboard update Glauber model are identical to those of the single-spin update model [14]. We have further shown that the analysis of Domany and Kinzel [5], for the ferromagnetic critical point at $J = \infty$, is equivalent to our formulation of the model.

5. Conclusion

By an explicit mapping (20) we have shown that the parameter space of the checkerboard Glauber model (with $\alpha = \frac{1}{2}$ and $\delta = 0$) is equivalent to a subspace of the full parameter space of the triangular cellular automata. As (2) is the most general form of the one-dimensional Ising Hamiltonian consistent with a mapping onto a triangular Ising model, we claim to have found the *only* subspace of the triangular cellular automata that obeys detailed balance. Furthermore, from the known equilibrium properties of the one-dimensional Ising model we have argued that there are no phase transitions within the interior of the cubical parameter space of the triangular cellular automata.

Because the Glauber model is embedded within the triangular cellular automata, we expect the phase transitions of the one-dimensional Ising model also to be represented in this cellular automata. Along with the ferromagnetic transition, which was studied by Domany and Kinzel in the context of the generalized directed percolation models, we find a new line of critical points associated with the zero-temperature antiferromagnetic Ising model in an external field. Using that the zero-field Glauber model is equivalent to the anisotropic triangular Ising antiferromagnetic at its disorder point, the results found by Stephenson imply the existence of a null-cone (29) for the correlation functions in the associated Glauber model. Because this null-cone results from the underlying properties of the checkerboard update procedure, we draw the conclusion that the entire triangular cellular automata exhibits this null-cone structure.

We have studied the critical properties of the checkerboard Glauber model. Our results along the path $J = \infty$ and $|H| \to 0$ are consistent with those of Domany and Kinzel. We have also shown that the checkerboard and single-spin update models have identical critical properties. Though we have only considered the $q = 2$ Glauber model,

our results can be generalized to arbitrary integer values of $q \geq 2$. This extension has been treated previously by Choi and Huberman [3] within the context of the q-state triangular cellular automata.

Finally we note that the restriction to the special case of $\alpha = \frac{1}{2}$ and $\delta = 0$ of the general Glauber model was imposed to simplify the discussion and to make contact with previous work in this area. The generalization to other choices of α and δ, which in general produces a mapping onto a square-lattice Ising model is currently underway.

Acknowledgments

I am grateful to M Schick for drawing my attention to this interesting subject and for many useful discussions. I also thank M den Nijs for several illuminating discussions. I also would like to acknowledge the hospitality of the Institut fur Physik at the Johannes-Gutenberg Universitat (at the invitation of K Binder) while this work was being completed.

References

[1] Glauber R 1963 *J. Math. Phys.* **4** 294
[2] Stanley H 1971 *Introduction to Phase Transitions and Critical Phenomenon* (Oxford: Oxford University Press)
[3] Choi M and Huberman B 1984 *J. Phys. A: Math. Gen.* **17** L765
[4] Wolfram S 1983 *Rev. Mod. Phys.* **55** 601
[5] Domany E and Kinzel W 1984 *Phys. Rev. Lett.* **53** 311
[6] Verhagen A 1976 *J. Stat. Phys.* **15** 219
[7] Enting I 1977 *J. Phys. C: Solid State Phys.* **10** 1379
[8] Domany E 1984 *Phys. Rev. Lett.* **52** 871
[9] Stephenson J 1970 *Can. J. Phys.* **48** 2118; 1970 *J. Math. Phys.* **11** 420
[10] Tang S and Landau D 1987 *Phys. Rev.* B **36** 567
[11] Van Kampen N 1981 *Stochastic Processes in Physics and Chemistry* (Amsterdam: North-Holland)
[12] Kinzel W 1985 *Z. Phys.* B **58** 229
[13] Cordery R, Sarker S and Tobochnik J 1981 *Phys. Rev.* B **24** 5402
[14] Haake F and Thol K 1980 *Z. Phys.* B **40** 219
[15] Peschel I and Emery V 1981 *Z. Phys.* B **43** 241
[16] Blöte H and Hilhorst H 1982 *J. Phys. A: Math. Gen.* **15** L631
[17] Pokrovsky V and Talapov A 1979 *Phys. Rev. Lett.* **42** 65
[18] den Nijs M 1988 *Phase Transitions and Critical Phenomena* vol 12 ed C Domb and J L Lebowitz (New York: Academic Press)
[19] Vichniac G 1984 *Physica* **10D** 96
[20] Kasteleyn P 1963 *J. Math. Phys.* **4** 287
Montroll E, Potts R and Ward J 1963 *J. Math. Phys.* **4** 308
Stephenson J 1964 *J. Math. Phys.* **5** 1009
[21] Hohenberg P and Halperin B 1977 *Rev. Mod. Phys.* **49** 435